Evidence for sortilin modulating regional accumulation of human tau prions in transgenic mice

Noah R. Johnson[a,1], Carlo Condello[a,b,1], Shenheng Guan[c], Abby Oehler[a], Julia Becker[a], Marta Gavidia[a], George A. Carlson[a,b], Kurt Giles[a,b], and Stanley B. Prusiner[a,b,d,2]

[a]Institute for Neurodegenerative Diseases, Weill Institute for Neurosciences, University of California, San Francisco, CA 94158; [b]Department of Neurology, University of California, San Francisco, CA 94158; [c]Department of Pharmaceutical Chemistry and Mass Spectrometry Facility, University of California, San Francisco, CA 94158; and [d]Department of Biochemistry and Biophysics, University of California, San Francisco, CA 94158

Contributed by Stanley B. Prusiner, November 8, 2017 (sent for review October 5, 2017; reviewed by Neil R. Cashman and Karen E. Duff)

Misfolding of tau proteins into prions and their propagation along neural circuits are thought to result in neurodegeneration causing Alzheimer's disease, progressive supranuclear palsy, chronic traumatic encephalopathy, and other tauopathies. Little is known about the molecular processes mediating tau prion replication and spreading in different brain regions. Using transgenic (Tg) mice with a neuronal promoter driving expression of human mutant (P301S) tau, we found that tau prion formation and histopathologic deposition is largely restricted to the hindbrain. Unexpectedly, tau mRNA and protein levels did not differ between the forebrain and hindbrain, suggesting that other factors modulating the conversion of tau into a prion exist and are region specific. Using a cell-based prion propagation assay, we discovered that tau prion replication is suppressed by forebrain-derived inhibitors, one of which is sortilin, a lysosomal sorting receptor. We also show that sortilin expression is higher in the forebrain than the hindbrain across the life span of the Tg mice, suggesting that sortilin, at least in part, inhibits forebrain tau prion replication in vivo. Our findings provide evidence for selective vulnerability in mice resulting in highly regulated levels of tau prion propagation, thus affording a model for identification of additional molecules that could mitigate the levels of tau prions in human tauopathies.

Alzheimer's disease | tau | prion | selective vulnerability | neurodegeneration

Misfolding and aggregation of the microtubule-associated protein tau underlies a variety of progressive neurodegenerative diseases, including Alzheimer's disease (AD), the frontotemporal dementias, and chronic traumatic encephalopathy. Misfolded tau self-assembles into oligomers and aggregates that can spread to naïve cells and continue self-templated propagation on intracellular tau (1). Each human tauopathy has a unique clinicopathologic phenotype defined by the types of tau deposits as well as the brain regions, cells, and behaviors they affect. Distinct pathogenic strains encoded by the structural conformations of tau have been suggested to underlie these diverse phenotypes, which are maintained upon serial transmission in vivo (2, 3). Thus, tau fulfills the defining criteria of a prion (4–6).

To understand the phenotypic diversity among progressive tauopathies, there has been considerable effort to elucidate the mechanisms of tau prion propagation. A wealth of evidence indicates that tau prions can move from cell to cell along defined neural pathways to produce the stereotyped regional progression of tauopathy observed in AD and other neurodegenerative diseases (7, 8). There is also compelling evidence that certain brain regions, or populations of cells within those regions, are predisposed to tau pathology, or are "selectively vulnerable" (9). Notably, brain regions highly affected by tau pathology in AD are acquired during the later stages of ontogenic development and have greater neuroplasticity than spared regions (10). Furthermore, these regions were recently found to contain unique gene expression profiles, indicating disrupted protein homeostasis before clinical symptoms (11). It thus appears likely that selective vulnerability and cell-to-cell pathogenic spreading together determine the spatiotemporal progression of human tauopathy. Careful evaluation of the biochemical context in which tau prion conversion initiates and proceeds, and where it is prohibited, is necessary to elucidate the role that each mechanism plays in this complex process.

Transgenic (Tg) mice expressing human tau with disease-causing familial mutations are commonly employed to study spontaneous tau aggregation in vivo, which does not occur by expression of wild-type (WT) human tau protein (12). The P301S mutation reduces tau's ability to stabilize microtubule assembly in vitro, increases its propensity to aggregate (13), and causes early onset frontotemporal dementias in humans (14). We used mice expressing 0N4R human tau with the P301S mutation driven by the mouse *Thy1* promoter, line B6-Tg(Thy1-MAPT*P301S)2541 (15), referred to herein as Tg2541 mice. We describe the unexpected finding that tau pathogenesis develops in a distinct spatiotemporal manner in the Tg2541 mouse brain that does not follow the regional pattern of transgene expression. Our results indicate that the tau prion cascade is influenced by the local microenvironment, revealing an intrinsic regional vulnerability to tau propagation in the hindbrain of these mice.

Significance

Human neurodegenerative diseases such as Alzheimer's disease develop in a highly stereotyped fashion, suggesting intrinsic differences among brain regions determine whether they are affected or spared. Here, we employed a widely used line of transgenic (Tg) mice expressing mutant (P301S) human tau and exhibiting robust tauopathy. By examining brain regions affected by and spared of tau prions, we found that localization of human tau prion formation in Tg mice arises from regional inhibition of tau prion replication. Using a cell-based bioassay, we identified an inhibitor of tau prion propagation in the forebrain. These discoveries may lead to the identification of key mediators of brain vulnerability involved in human tauopathies, a promising strategy for the development of targeted therapeutics for these diseases.

Author contributions: N.R.J., C.C., S.G., K.G., and S.B.P. designed research; N.R.J., C.C., S.G., A.O., J.B., and M.G. performed research; N.R.J., C.C., and S.G. analyzed data; and N.R.J., C.C., G.A.C., K.G., and S.B.P. wrote the paper.

Reviewers: N.R.C., University of British Columbia; and K.E.D., Columbia University Medical Center.

Conflict of interest statement: The Institute for Neurodegenerative Diseases, University of California, San Francisco has a research collaboration with Daiichi Sankyo (Tokyo, Japan). S.B.P. is the chair of the Scientific Advisory Board of Alzheon, Inc., which has not contributed financial or any other support to these studies.

[1]N.R.J. and C.C. contributed equally to this work.

[2]To whom correspondence should be addressed. Email: stanley.prusiner@ucsf.edu.

This article contains supporting information online at www.pnas.org/lookup/suppl/doi:10.1073/pnas.1717193114/-/DCSupplemental.

Results

Tau Pathology Is Localized to the Hindbrain of Tg2541 Mice. Building on previous work (15–17), we first determined the time course of phosphorylated tau (pTau) pathology in the brains of Tg2541 mice using the antibody AT8 (pS202/pT205). Immunofluorescence staining of 180-d-old Tg2541 mice revealed a clear rostrocaudal difference, with numerous tau pathologies in the brainstem and midbrain structures and far fewer in the cerebral cortex (Fig. 1*A*). Pathological features included circumscribed inclusions, granular inclusions, and homogeneous staining of the cell body and neuropil threads. We grouped forebrain structures and hindbrain structures (Fig. 1*B*) and found significantly greater tau pathology in the hindbrain compared with the forebrain beginning at 120 d of age (Fig. 1*C*). Tau phosphorylation at a second epitope (S396/S404) was also elevated in the hindbrain of mice beyond 120 d of age, measured by ELISA (Fig. 1*D*) and Western blot (Fig. 1*E*).

Human Tau Protein Is Uniformly Expressed in the Tg2541 Mouse Brain. We next evaluated whether transgene expression levels were responsible for the regional difference in histopathological pTau deposition. Human tau mRNA was measured by quantitative RT-PCR (qRT-PCR), and, unexpectedly, the gene expression levels were similar in the forebrain and hindbrain of 30-, 90-, and 180-d-old mice (Fig. 2*A*). Messenger RNA levels of endogenous mouse tau were also similar in the forebrain and hindbrain and were at least 10-fold lower in expression compared with human tau in both regions. Measuring human tau by Western blot, we found comparable protein levels in the forebrain and hindbrain of Tg2541 mice, presumably increasing with age due to accumulation of tau aggregates (Fig. 2*B*). To evaluate regional protein expression in greater detail, immunofluorescence staining for total human tau protein was performed. Human tau expression was observed in a subset of cells in all brain regions, although in greater numbers in regions such as the thalamus,

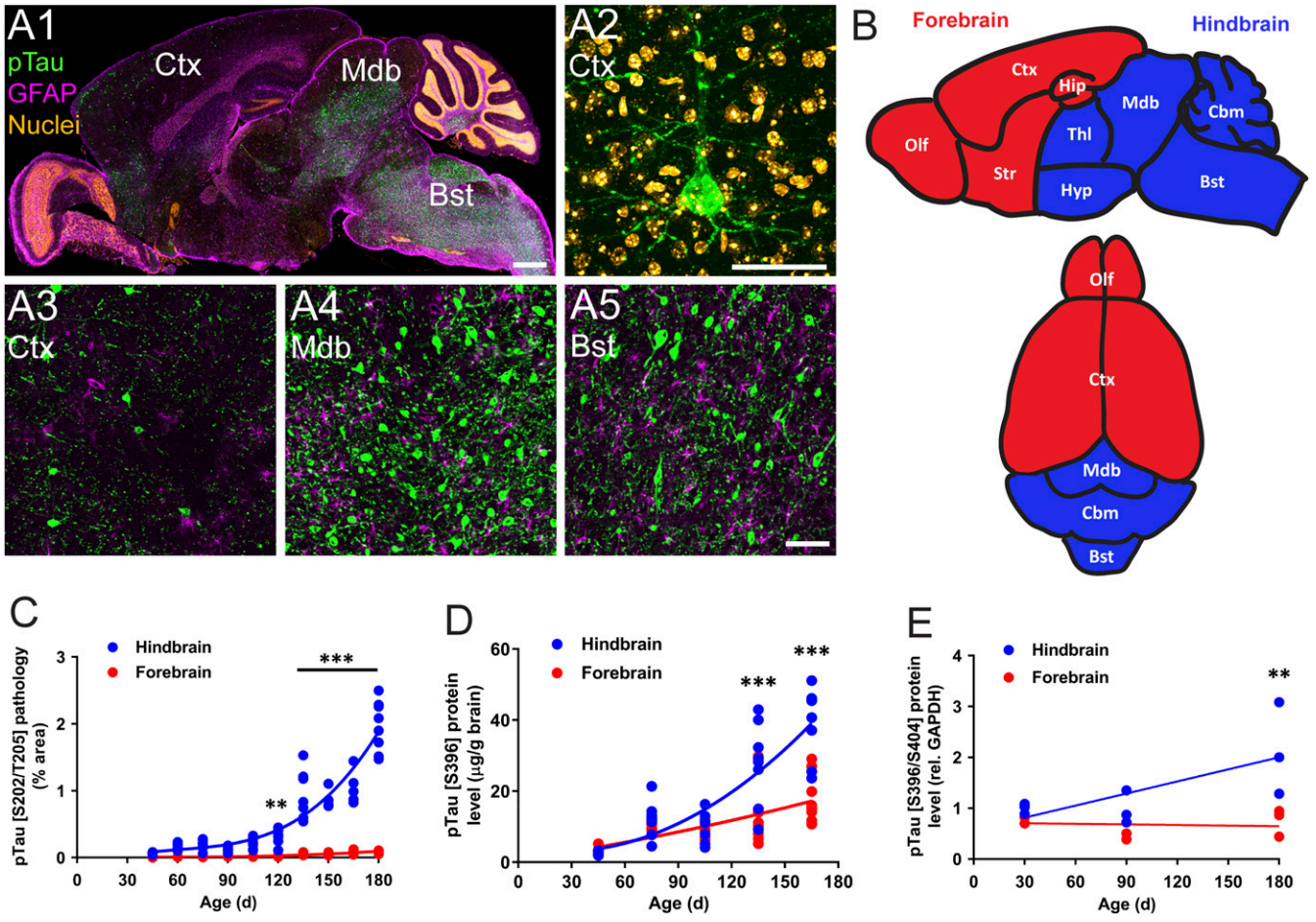

Fig. 1. Hindbrain localization of pTau pathology in Tg2541 mice. (*A*, *1*) Representative immunofluorescence staining of a 180-d-old Tg2541 mouse brain for pTau (AT8 antibody, green), glial fibrillary acidic protein (GFAP, pink), and cell nuclei (propidium iodide, orange) revealing the predominance of tau pathology in the brainstem and midbrain. (Scale bar, 1,000 μm.) (*A*, *2*) High magnification image of a single tau-filled neuron in the cortex (Ctx) with pTau (green) and nuclei (orange). (Scale bar, 30 μm.) (*A*, *3*–*A*, *5*) Magnified images of pathology in the cortex (Ctx), midbrain (Mdb), and brainstem (Bst) with pTau (green) and GFAP (pink). (Scale bar, 100 μm.) (*B*) Sagittal (*Top*) and dorsal (*Bottom*) views of the mouse brain separated into two regions: forebrain (red), which included the cortex (Ctx), hippocampus (Hip), striatum (Str), and olfactory bulb (Olf), and the hindbrain (blue), which included the brainstem (Bst), cerebellum (Cbm), midbrain (Mdb), thalamus (Thl), and hypothalamus (Hyp). (*C*) Quantitative immunofluorescence analysis revealed a significantly higher percent area of pTau pathology (AT8 antibody) in the Tg2541 hindbrain compared with the forebrain starting at 120 d of age ($n = 5$–8 mice per age; $^{**}P = 0.003$; $^{***}P < 0.001$). (*D*) ELISA analysis showing significantly increased levels of pTau protein (pS396 antibody) in the Tg2541 hindbrain compared with the forebrain beginning at 135 d of age ($n = 7$–8 mice per age; data normalized to brain weight; $^{***}P < 0.001$). (*E*) Immunoblot analysis indicating significantly higher pTau [S396/S404] protein in the Tg2541 hindbrain compared with the forebrain at 180 d of age ($n = 3$ mice per age; data normalized to GAPDH levels; $^{**}P = 0.005$). (*C*–*E*) Each mouse is shown as an individual data point, and forebrain and hindbrain were compared at each age by two-way ANOVA, followed by Bonferroni's multiple comparisons post hoc testing.

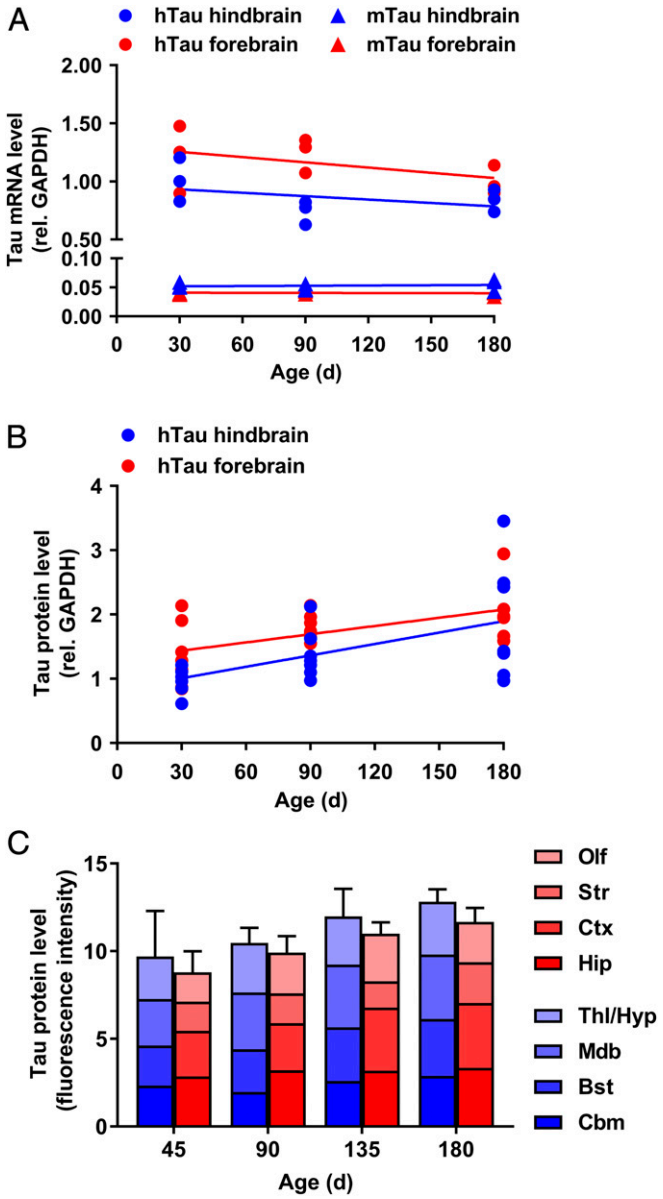

Fig. 2. Tau expression levels are similar in the forebrain and hindbrain of Tg2541 mice. (*A*) qRT-PCR analysis of mRNA transcript levels for human and mouse tau in the hindbrain and forebrain of Tg2541 mice, relative to GAPDH mRNA levels and normalized to hindbrain expression level at 30 d of age ($n = 3$ mice per age; $P > 0.05$). (*B*) Quantification of Western blot analysis of total human tau protein (Tau13 antibody) in the Tg2541 hindbrain and forebrain relative to GAPDH levels and normalized to hindbrain protein level at 30 d of age ($n = 7$ mice per age; $P > 0.05$). (*C*) Quantification of immunofluorescence staining for total human tau (Tau13 antibody) reported as summed fluorescence intensity of regions in the hindbrain (blue shades) and forebrain (red shades). Each region was corrected for background fluorescence intensity using the same staining conditions with WT mice ($n = 3$ mice per age; $P > 0.05$). Data represent mean ± SD of summed fluorescence intensities of forebrain or hindbrain regions, compared at each age by two-way ANOVA, followed by Bonferroni's multiple comparisons post hoc testing. (*A* and *B*) Each mouse is shown as an individual data point, and forebrain and hindbrain were compared at each age by two-way ANOVA, followed by Bonferroni's multiple comparisons post hoc testing.

midbrain, and cortex (Fig. S1). However, when the fluorescence intensities of the individual brain regions were summed and corrected for background fluorescence in WT mice, there was no difference in cumulative tau protein level between the forebrain and hindbrain at any age (Fig. 2*C*). Taken together, these results indicate that transgene expression is not higher in the hindbrain of Tg2541 mice compared with the forebrain and, therefore, does not explain the hindbrain predominance of pTau pathology.

Human Tau Prions Selectively Accumulate in the Hindbrain of Tg2541 Mice. We next employed a cell-based assay sensitive to self-templating tau species to determine whether the time course of

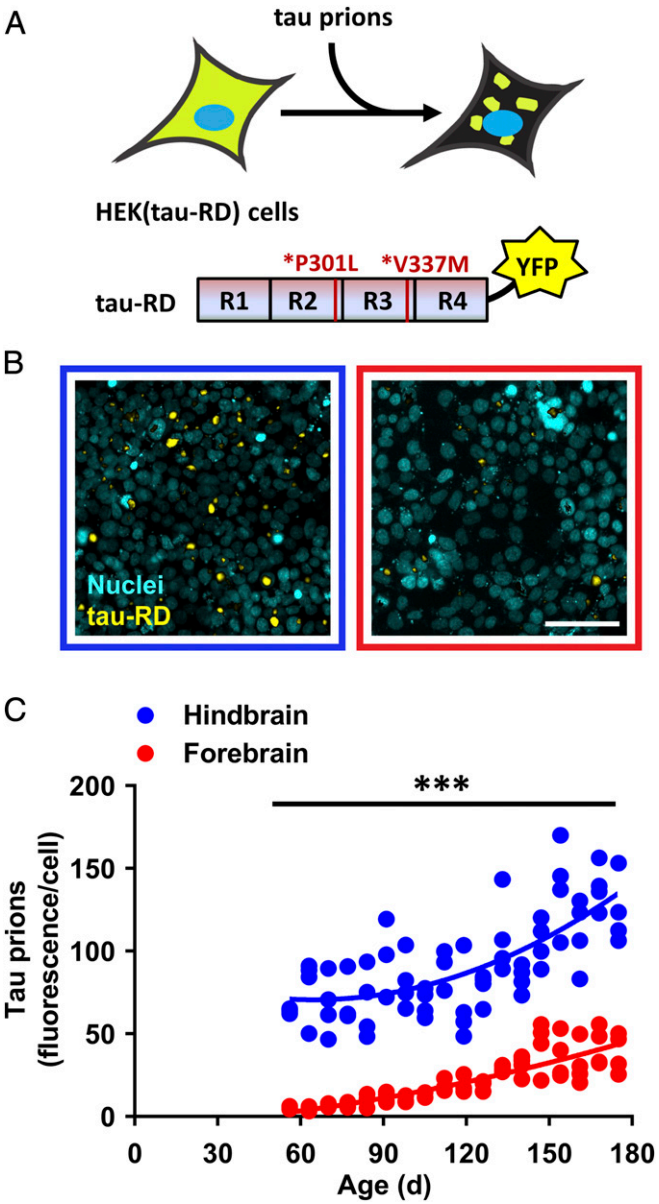

Fig. 3. Tau prions are localized to the hindbrain of Tg2541 mice. (*A*) Schematic of the in vitro tau prion assay using HEK cells expressing tau-RD. YFP signal is diffuse until tau prions are added, inducing intracellular tau-RD aggregation, which is measured by high-content confocal analysis. (*B*) HEK cells treated with Tg2541 mouse hindbrain lysate (blue border) results in a much greater number of fluorescent tau aggregates (yellow) per cell nuclei (blue) than forebrain lysate (red border). (Scale bar, 50 μm.) (*C*) Quantification of tau prions measured as fluorescence intensity of tau aggregates per cell, revealing significantly greater numbers of tau prions in the Tg2541 hindbrain compared with the forebrain at all ages from 56 to 175 d ($n = 4$ mice per age; $^{***}P < 0.001$). Each mouse is shown as an individual data point, and forebrain and hindbrain were compared at each age by two-way ANOVA, followed by Bonferroni's multiple comparisons post hoc testing.

pTau pathology reflected the biological activity of tau prions in the forebrain and hindbrain. The cell model used was originally developed to identify tau prions in the brains of human tauopathy patients (2) and was then adapted to a high-content confocal analysis system (18). Human embryonic kidney (HEK) cells that express the repeat domain of tau (tau-RD) with two point mutations and fused to yellow fluorescent protein (YFP) were used [originally called Tau(4RD*LM)–YFP (2) cells but herein referred to simply as HEK(tau-RD) cells]. Tau prions derived from brain lysate can enter HEK(tau-RD) cells and initiate tau aggregation (Fig. 3*A*), measured here as the total fluorescence intensity of aggregates per cell.

To measure the levels of tau prions in the brains of Tg2541 mice, the forebrain and hindbrain were separated via the natural fold below the cerebral cortex, and a single cut was made between the hypothalamus and striatum. Both forebrain and hindbrain lysates from a 180-d-old mouse resulted in tau aggregation within HEK(tau-RD) cells, indicating that replicating tau prions were present in both regions. Hindbrain lysate, however, induced a much greater number of aggregates than did the forebrain lysate (Fig. 3*B*). Measuring lysates from Tg2541 mice of different ages showed that tau prions were present in the hindbrain at significantly higher levels compared with the forebrain, occurring in mice as young as 56 d of age and increasing throughout life (Fig. 3*C*). The presence of biologically active tau prions at least 2 mo before neuropathologically measureable tau deposits suggests that tau prions precede tau hyperphosphorylation and aggregation. These data provide compelling evidence of a regional vulnerability to tau prion formation in the brains of Tg2541 mice.

Tau Phosphorylation Is Region Specific. Posttranslational processing of tau has been shown to influence the stability of microtubules, and some posttranslational modifications (PTMs) have been implicated in its gain-of-neurotoxic function (10, 19, 20). Given the significant difference in tau prion levels in 90-d-old Tg2541 mice, despite similar levels of tau phosphorylation detected by antibodies (Fig. 1 *C*–*E*), we turned to high-resolution mass spectrometry to evaluate other PTMs of tau. Tau phosphorylation was detected at four sites (Fig. 4*A*), and relative levels were quantified by spectral counting (Fig. 4*B*). Similar levels of phosphorylation in the forebrain and hindbrain at S202/T205 and S404 were observed, confirming our pTau immunohistochemistry and Western blot data. Phosphorylation at T181 was also detected, although at very low abundance. Interestingly, phosphorylation at S412/S413/T414 was only detected in the forebrain. We hypothesize that this PTM might be protective against tau prions, producing a structure unfavorable to templating. Our data, however, suggest a tau PTM is unlikely to be the primary cause underlying the regional distribution of tau prions in Tg2541 mice. Ninety days of age is the midpoint of the Tg2541 mouse life span, and evaluation earlier or later in life may reveal the temporal regulation of tau processing and its relationship to tissue vulnerability at different disease stages.

Endogenous Mouse Tau Inhibits Propagation of Human Tau Prions. Suppressed propagation of human prions by their endogenous counterpart has been observed previously in Tg mice expressing the human prion protein (PrP) (21) and human α-synuclein (22). We generated Tg2541 *Mapt*$^{0/0}$ mice by backcrossing to a line lacking endogenous tau expression (23). Ablation of the mouse tau gene did not alter survival of Tg2541 mice (Fig. 5*A*), yet it did accelerate tau prion replication, with significantly higher levels detected in the hindbrain of mice more than 120 d old and in the forebrain of 180-d-old mice (Fig. 5*B*). These findings indicate that mouse tau acts as an inhibitor of human tau prion replication in the Tg2541 mouse brain. However, since the expression of mouse tau and its inhibitory effect is similar in both the forebrain and hindbrain, it is insufficient to explain the regional formation of tau prions.

Because Pin1, a peptidyl-prolyl isomerase that acts on phospho(Ser/Thr)-Pro motifs, has been proposed to maintain the

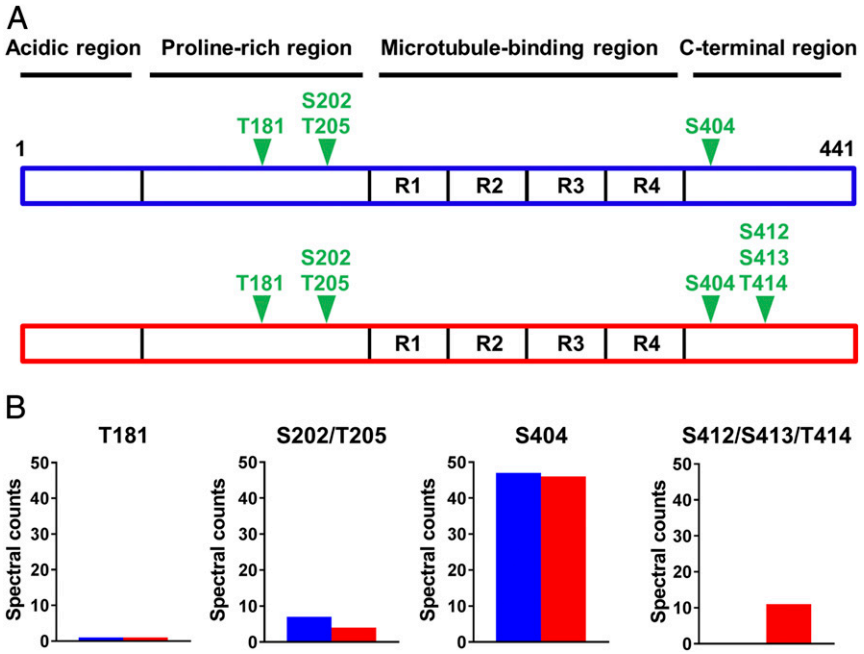

Fig. 4. Tau phosphorylation in the hindbrain and forebrain of Tg2541 mice. (*A*) Hindbrain (blue) or forebrain (red) lysates from 90-d-old Tg2541 mice were analyzed by mass spectrometry for PTMs of tau. Phosphorylated epitopes are shown labeled at the modified residue in full-length human tau. Multiple residues are listed together if phosphorylation could not be unambiguously assigned to a single site. (*B*) Quantification of tau phosphorylation levels at each epitope by spectral counting. Data show the sum of spectra from two technical replicates from each of three different mice.

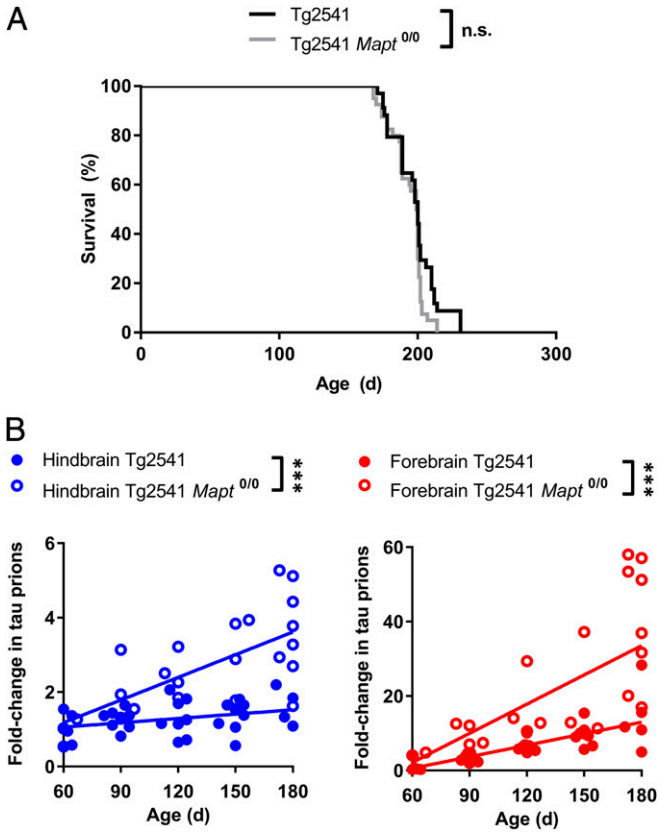

Fig. 5. Endogenous mouse tau inhibits human tau prion propagation. (*A*) Crossing Tg2541 mice with a strain lacking endogenous mouse tau did not have a significant effect on disease onset ($n = 34$ for Tg2541; $n = 39$ for Tg2541 *Mapt*$^{0/0}$; n.s., not significant, $P = 0.076$ by log-rank Mantel–Cox test). (*B*) Tg2541 mice lacking endogenous mouse tau had significantly increased levels of tau prions in the hindbrain and forebrain compared with normal Tg2541 mice, as detected using HEK(tau-RD) cells. Data were normalized to the 60-d-old Tg2541 group and reported as fold change ($n = 4$–10 mice per age; ***$P < 0.001$, asterisks shown vertically). Each mouse is shown as an individual data point, and linear regression was used to determine whether the slopes of the best-fit lines were significantly different.

tau protein in a stable and nonpathogenic conformation (24), we evaluated this possibility. When Tg2541 mice were crossed with a line lacking Pin1, we found no significant effect on the levels of total tau protein, or tau prion levels in the hindbrain or forebrain (Fig. S2). Given that PTMs of Pin1 modulate its activity and are deregulated by tau overexpression (25), we are unable to draw conclusions about the function of Pin1 in a normal physiological setting. However, Pin1 does not contribute to the regional vulnerability to tau propagation in Tg2541 mice.

Inhibitors of Tau Prion Replication Exist in the Tg2541 Mouse Forebrain. We next considered whether inhibitory factors besides mouse tau might be responsible for the low levels of tau prions in the forebrain. We used HEK(tau-RD) cells to measure the ability of forebrain lysates to inhibit tau prions from the hindbrains of Tg2541 mice. We tested forebrain lysates from 30- or 180-d-old Tg2541 mice, or WT mice as a control, adding increasing concentrations to decreasing concentrations of hindbrain lysate to maintain an equivalent amount of total protein added to the cells. Compared with the normal dilution curve of hindbrain lysate alone, forebrain lysate from Tg2541 mice inhibited tau aggregation in the cells, in contrast to WT mouse lysate, which showed no inhibition (Fig. 6*A*). Furthermore, we observed greater inhibitory activity of forebrain lysate derived from 30-d-old mice compared with 180-d-old mice, consistent with their age-dependent progression of tauopathy. These data suggest the possibility of inhibitors of tau prion replication in the forebrains of Tg2541 mice.

Sortilin Is an Inhibitor of Human Tau Prion Replication. Stimulated by a recent report that the lysosomal sorting receptor sortilin mediates lysosomal degradation of PrP (26), and its established role in amyloid-β (Aβ) (27) and TDP-43 proteinopathies (28), we investigated its potential involvement with tau. When four different sortilin antibodies were mixed with forebrain homogenate, they each blocked its ability to inhibit hindbrain-derived tau prions in a dose-dependent manner, whereas a GAPDH control antibody did not (Fig. 6*B*). In contrast, antibodies against progranulin or transmembrane protein 106B (TMEM106B), also involved in lysosomal regulation (29, 30), had no effect on forebrain inhibition. As a positive control, an antibody against pTau also directly inhibited hindbrain-derived tau prions (Fig. S3). Therefore, sortilin is one inhibitor of human tau prion replication, and sortilin-mediated lysosomal degradation may play an important role in tau prion formation and clearance. We found sortilin gene expression

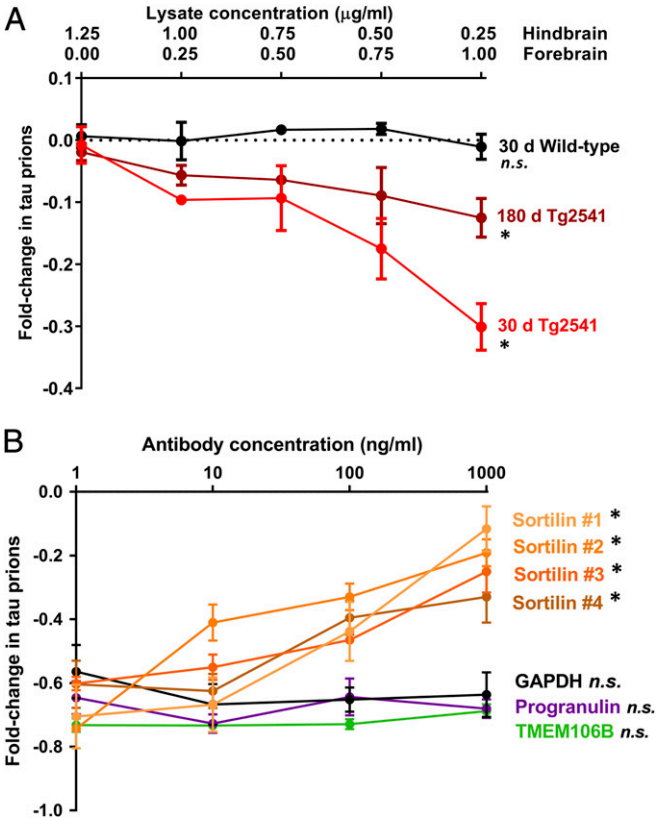

Fig. 6. Tg2541 forebrain contains inhibitors of tau prion replication. (*A*) Forebrain lysate from 30- or 180-d-old Tg2541 mice or 30-d-old WT mice was mixed into hindbrain lysate pooled from 180-d-old Tg2541 mice, and tau prions were measured using HEK(tau-RD) cells. Data were normalized to pooled hindbrain lysate alone at each concentration and presented as fold change ($n = 3$ mice per group; n.s., not significant, $P = 0.758$; *$P < 0.05$). (*B*) Antibodies were used to neutralize the function of various proteins in 30-d-old Tg2541 forebrain lysate (1 μg/mL), then combined with 180-d-old Tg2541 hindbrain lysate (0.25 μg/mL), and tau prions were measured using HEK(tau-RD) cells. Neutralizing sortilin blocked the inhibitory function of forebrain lysate ($n = 6$ wells per group; *$P < 0.05$), while antibodies against progranulin, TMEM106B, or GAPDH had no effect (n.s., not significant, $P > 0.05$). (*A* and *B*) Data represent mean ± SD, and linear regression was used to determine whether the slopes of the best-fit lines were significantly nonzero.

and protein levels to be significantly higher in the forebrain compared with the hindbrain of Tg2541 mice throughout their life span (Fig. 7 *A* and *B*), and levels of progranulin were increased in the forebrain as well (Fig. S4*A*). However, sortilin protein levels were also higher in the forebrain compared with the hindbrain of WT mice (Fig. S4*B*), indicating that sortilin is unlikely to be the only factor inhibiting tau prion propagation in the Tg2541 mouse brain. The mechanistic details of sortilin inhibition of human tau prions remain to be established.

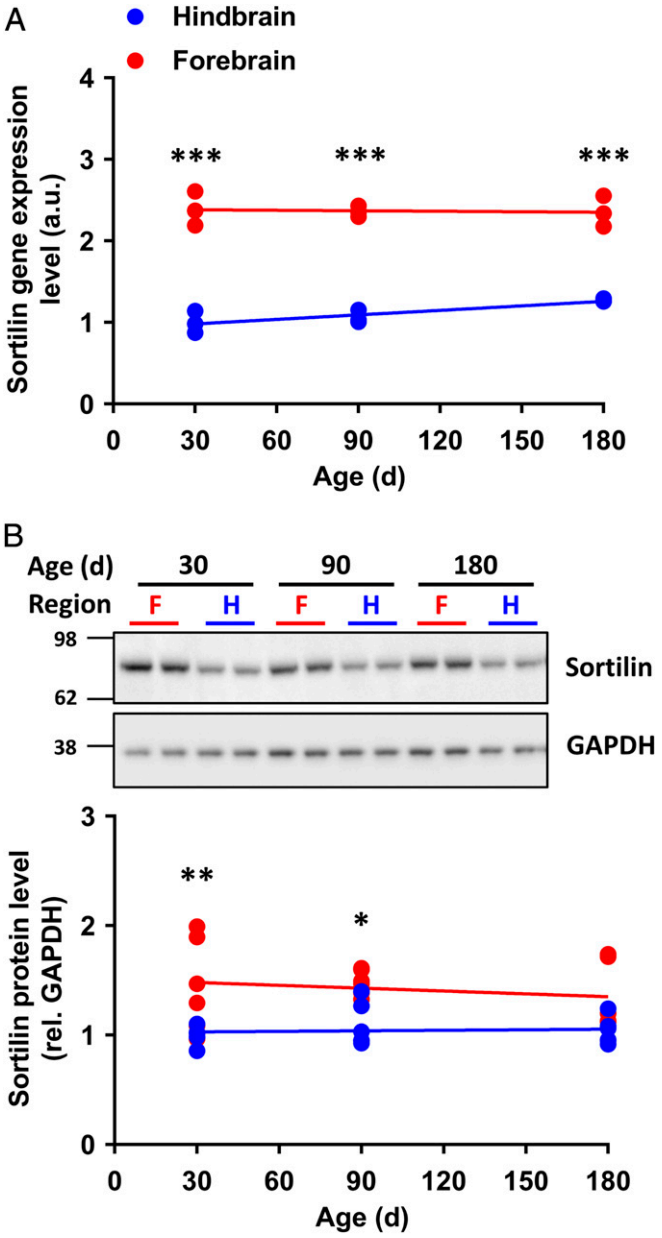

Fig. 7. Sortilin expression is higher in the Tg2541 forebrain. (*A*) Sortilin gene expression in the hindbrain and forebrain of Tg2541 mice, relative to housekeeping gene levels and normalized to hindbrain expression level at 30 d of age ($n = 3$ mice per age; $^{***}P < 0.001$). (*B*) Western blot analysis of sortilin in the Tg2541 hindbrain (H, blue) and forebrain (F, red). Band intensities were quantified relative to GAPDH levels and normalized to the hindbrain protein level at 30 d of age ($n = 6$ mice per age; $^{**}P = 0.009$; $^{*}P = 0.024$). (*A* and *B*) Each mouse is shown as an individual data point, and forebrain and hindbrain were compared at each age by two-way ANOVA, followed by Bonferroni's multiple comparisons post hoc testing.

Discussion

Although Tg2541 mice were developed 15 y ago, the implications of the regional pattern of pathological tau deposition in their brains have thus far been overlooked, to our knowledge. Here, we uncover a selective vulnerability to tau prion propagation and examine the underlying cause. We found that the region-specific accumulation of tau prions, followed by pTau deposition, was independent of transgene expression levels. These findings are consistent with the global expression pattern of the endogenous *Thy1* promoter throughout the central nervous system from embryonic day 11 (31). In AD, the earliest tau pathology is observed in select subcortical nuclei (32), many of which are analogous to hindbrain structures in Tg2541 mice. Similarly, in Parkinson's disease, Lewy bodies made up of α-synuclein originate in the brainstem, then progress to the midbrain and neocortex with age (33). Interestingly, TgM83$^{+/+}$ mice expressing mutant human α-synuclein, which develop α-synuclein prions spontaneously at about 400 d of age (34–36), show neuropathological inclusions first in the brainstem and deep cerebellar nuclei with sparse pathology in the cerebral cortex (37). The selective vulnerability observed in Tg2541 mice may therefore play a role in a spectrum of diseases caused by neuropathogenic prions.

We observed that ablation of endogenous mouse tau accelerated replication of human tau prions in Tg2541 mice. Consistent with our findings, knocking out endogenous tau has been shown to accelerate tau pathology in two other Tg mouse models (38, 39). Reduced structural competency of endogenous tau for templating, particularly due to low sequence similarity in the N-terminal acidic domain and differing PTMs, has been proposed as one possible mechanism by which mouse tau interferes with human tau propagation (39). The converse has also been reported in mice expressing high levels of P301L human tau in the forebrain. Ablation of endogenous tau had no effect on tau pathology but reduced the neurotoxic effects of mutant human tau (40). However, we found expression of mouse tau to be low compared with that of human tau in Tg2541 mice, and tau in the WT mouse forebrain did not exhibit an inhibitory effect in our HEK(tau-RD) cell experiments. We conclude that mouse tau can interfere with the propagation of human tau prions in vivo, but it is not the primary mechanism of selective vulnerability in Tg2541 mice.

Sortilin is a member of the vacuolar protein sorting-10 protein (VPS10P) receptor family containing type-1 transmembrane proteins that have pleiotropic functions in neuronal protein trafficking and viability (41). VPS10P-domain receptors regulate intracellular processing of amyloid precursor protein (APP) (42, 43) and β-secretase (44), which cleaves APP to produce neurotoxic Aβ peptides. Sortilin also plays a role in frontotemporal lobar degeneration (FTLD) by binding and regulating extracellular concentrations of the secreted glycoprotein progranulin (28). Progranulin deficiency due to mutation causes inherited FTLD with ubiquitin and TDP-43 inclusions (45–47). Most recently, the sortilin receptor has been shown to bind PrP and shuttle it to the lysosome for degradation (26). Sortilin knockout accelerated prion disease in PrP-infected mice. Furthermore, PrP-infected cells had increased lysosomal degradation of sortilin alone or complexed with PrP, a potential mechanism by which PrP accumulates in neurons (26). Here, we report that sortilin also plays a role in tau prion replication and may thus represent an exciting target for therapeutic intervention in tau-related diseases.

Materials and Methods

Animals. The Tg2541 line was originally generated on a mixed C57BL/6J × CBA/Ca background (15) and bred onto a C57BL/6J background using marker-assisted backcrossing for eight generations before intercrossing to generate homozygous congenic mice. Knockout mice were generated by intercrossing Tg2541 with C57BL/6J lines lacking endogenous mouse tau (23) or endogenous Pin1 (48). Animals were maintained in a facility accredited by

the Association for Assessment and Accreditation of Laboratory Animal Care International in accordance with the *Guide for the Care and Use of Laboratory Animals* (49). All procedures for animal use were approved by the University of California, San Francisco's Institutional Animal Care and Use Committee.

Tissue Processing. Brains were removed and separated into forebrain and hindbrain pieces using a single cut with a razor blade between the striatum and hypothalamus. Tissue was homogenized in nine volumes of cold DPBS containing 1× Halt Protease and Phosphatase Inhibitor Mixture (Thermo Fisher Scientific) using a Precellys 24-bead beater (Bertin Instruments) with metal bead lysing matrix (MP Biomedical). Where necessary, brain lysates were clarified by centrifugation at 10,000 × *g* for 10 min at 4 °C. All tissue and samples were stored at −80 °C until further use.

Immunohistochemical Analysis. Brains were fixed in 10% neutral buffered formalin, paraffin embedded, and 8-μm sections were cut. Slides were deparaffinized in a 61 °C oven for 15 min and rehydrated through alcohols. Antigen retrieval was performed by autoclaving for 10 min at 121 °C in 0.01 M citrate buffer. Sections were blocked in 10% normal goat serum (NGS) (Vector Labs) for 1 h at room temperature. Sections were incubated with either the AT8 antibody (1:250; Thermo Fisher Scientific) to detect pTau pathology or the Tau13 antibody (1:1,000; produced in house) to detect total human tau. Primary antibodies were incubated in 10% NGS overnight at room temperature, then recognized with Alexa Fluor 488-conjugated goat anti-mouse IgG secondary antibody (1:500; Invitrogen) for 2 h at room temperature. Images were acquired with an Axio Scan.Z1 slide scanner (Zeiss), and quantification was performed with Zen 2.3 software (Zeiss).

Biochemical Analysis. Clarified brain lysates were normalized to a total protein concentration of 2 mg/mL and combined with NuPage LDS Sample Buffer and Reducing Agent (Invitrogen) and boiled for 10 min at 100 °C. A total of 10 μg protein was loaded per well in a 4–12% Bis-Tris gel and subjected to denaturing electrophoresis in Mops SDS buffer (Invitrogen). Gels were transferred to iBlot PVDF membranes (Invitrogen) and blocked in 5% BSA for 2 h at room temperature. Membranes were incubated overnight at 4 °C with primary antibodies Tau13 for total human tau (1:10,000; produced in house), PHF-1 for pTau [S396/S404] (1:1,000; a kind gift from Peter Davies, Feinstein Institute for Medical Research, Manhasset, NY), sortilin (1:500; Proteintech), progranulin (1:400; R&D Systems), or GAPDH (1:5,000; Abcam). HRP-conjugated secondary antibodies (1:10,000; Thermo Fisher Scientific) were incubated for 45 min, and membranes were developed with ProSignal Dura ECL substrate (Genesee Scientific) and imaged using a ChemiDoc Touch system (Bio-Rad).

To measure pTau concentration by ELISA, mouse brain lysates were first subjected to formic acid extraction. Twenty-five microliters lysate was combined with 50 μL formic acid and incubated for 20 min at 37 °C with sonication. Samples were then centrifuged at 100,000 × *g* for 1 h, and 50 μL supernatant was combined with 950 μL neutralization buffer (1 M Tris base; 0.5 M Na_2HPO_4). Samples were then diluted 1:10, and the human Tau [pSer396] ELISA kit (Invitrogen) was used according to the manufacturer's instructions.

HEK(Tau-RD) Cell Tau Aggregation Assays. HEK(tau-RD) cells were described previously (18). Briefly, HEK293T cells (ATCC) were transfected using Lipofectamine 2000 (Thermo Fisher Scientific) to express the RD of 4R human tau (aa 243–375) containing the P301L and V337M mutations and C-terminally fused to YFP. A stable monoclonal line was maintained in DMEM, supplemented with 10% FBS and 1% penicillin/streptomycin.

To measure tau prions in brain lysates, samples were clarified and total protein concentration was normalized. Lysate at a final concentration of 1.25 μg/mL total protein was first incubated with Lipofectamine 2000 (0.2% final concentration) and OptiMEM (9.8% final concentration) for 90 min, then added to 5,000 cells in each well of a 384-well plate. Plates were incubated at 37 °C for 3 d, then tau aggregates were imaged and quantified on an IN Cell Analyzer 6000 Cell Imaging System (GE Healthcare).

To measure inhibition of tau prions by forebrain lysates, hindbrain lysates from six 180-d-old male Tg2541 mice were pooled. Forebrain lysates from three 30-d-old or 180-d-old Tg2541 mice and three 30-d-old WT mice were tested. Lysates were diluted to final concentrations of 1.25, 1.00, 0.75, 0.50, and 0.25 μg/mL total protein, and each concentration of forebrain lysate was mixed with the corresponding concentration of pooled hindbrain lysate for a total concentration of 1.25 μg/mL protein and added to HEK(tau-RD) cells as described above. To examine the effect of neutralizing proteins in Tg2541 forebrain lysate, a 10-fold dilution series starting at 1 μg/mL final concentration of antibodies against sortilin (no. 1, Millipore; no. 2, BD Biosciences; no. 3, Proteintech; and no. 4, Abcam), progranulin (R&D Systems), TMEM106B (Novus Biologicals), pTau [S396/S404] (a kind gift from Peter Davies, Feinstein Institute for Medical Research, Manhasset, NY), and GAPDH (Abcam) were prepared. Each concentration was then combined with a 1.00 μg/mL final concentration of forebrain lysate pooled from three different 30-d-old Tg2541 mice, incubated at room temperature for 30 min, then combined with a 0.25 μg/mL final concentration of hindbrain lysate pooled from three different 180-d-old Tg2541 mice and added to HEK(tau-RD) cells as described above.

qRT-PCR Gene Expression Analysis. Total RNA was isolated from clarified brain lysates using the Quick-RNA MiniPrep kit (Zymo Research) following the manufacturer's instructions. qRT-PCR was performed using the Sensi-FAST SYBR Lo-ROX One-Step Kit (Bioline) following the manufacturer's instructions, using primers for human tau (Fwd, 5′-CCCAATCACTGCCTATACCC-3′ and Rev, 5′-CCACGAGAATGCGAAGGA-3′), mouse tau (Fwd, 5′-CCCCCTAAGTCACCATCAGCTAGT-3′ and Rev, 5′-CACTTTGCTCAGGTCCACCGGC-3′), and mouse GAPDH (Fwd, 5′-TGCCCCCATGTTGTGATG-3′ and Rev, 5′-TGTGGTCATGAGCCCTTCC-3′) as a control.

Nanostring Gene-Expression Analysis. Total RNA samples purified as described above were analyzed for sortilin gene expression using the nCounter system (Nanostring Technologies) following the manufacturer's instructions. Data analysis was performed using nSolver software (Nanostring Technologies).

Mass Spectrometry. In-solution digests were performed on lysates of the forebrain and hindbrain of three 90-d-old Tg2541 mice. Brain lysate containing 100 μg protein was solubilized in 8 M urea containing 100 mM ammonium bicarbonate and 1 mM EDTA. Samples were reduced with 10 mM DTT at 37 °C for 1 h with shaking, alkylated with 25 mM iodoacetamide at room temperature for 30 min in the dark, then quenched with 20 mM DTT. One milliliter ice-cold acetone was added and incubated at −20 °C for 1 h to precipitate proteins. Samples were centrifuged at 13,000 × *g* for 10 min at 4 °C, and the supernatant was carefully removed. Pellets were resuspended in 8 M urea, then diluted to 2 M using 100 mM ammonium bicarbonate buffer. Trypsin (500 ng) was added and incubated overnight at 37 °C with shaking. Digestion was stopped with formic acid, and 1 μg protein was analyzed by LC-MS/MS using an QExactive Plus (Thermo Fisher Scientific) mass spectrometer. Centroid peak lists were generated using in-house software (PAVA) and searched using Protein Prospector v. 5.19.1 (50). An expectation value cutoff of 1.0 E-6 was applied to only consider high-quality spectra, and identified spectra were then manually confirmed for accurate peak assignments. Quantification was performed by spectral counting, and the results from two LC-MS/MS technical replicates of each biological sample were summed.

Data Sharing Statement. All relevant data are presented in the manuscript and *Supporting Information*.

ACKNOWLEDGMENTS. We thank Dr. Michel Goedert for supplying the Tg2541 mice and Dr. Dale Hoyt for supplying the *Pin1*$^{0/0}$ mice. This work was supported by National Institutes of Health Grants AG002132 and AG031220, as well as by support from Daiichi Sankyo, the Henry M. Jackson Foundation, the Dana Foundation, the Glenn Foundation, the Mary Jane Brinton Fund, the Rainwater Charitable Foundation, and the Sherman Fairchild Foundation.

1. Goedert M (2016) The ordered assembly of tau is the gain-of-toxic function that causes human tauopathies. *Alzheimers Dement* 12:1040–1050.
2. Sanders DW, et al. (2014) Distinct tau prion strains propagate in cells and mice and define different tauopathies. *Neuron* 82:1271–1288.
3. Kaufman SK, et al. (2016) Tau prion strains dictate patterns of cell pathology, progression rate, and regional vulnerability in vivo. *Neuron* 92:796–812.
4. Goedert M (2015) Neurodegeneration. Alzheimer's and Parkinson's diseases: The prion concept in relation to assembled Aβ, tau, and α-synuclein. *Science* 349:1255555.
5. Prusiner SB (2012) Cell biology. A unifying role for prions in neurodegenerative diseases. *Science* 336:1511–1513.
6. Frost B, Diamond MI (2010) Prion-like mechanisms in neurodegenerative diseases. *Nat Rev Neurosci* 11:155–159.
7. Seeley WW, Crawford RK, Zhou J, Miller BL, Greicius MD (2009) Neurodegenerative diseases target large-scale human brain networks. *Neuron* 62:42–52.
8. Brettschneider J, Del Tredici K, Lee VM-Y, Trojanowski JQ (2015) Spreading of pathology in neurodegenerative diseases: A focus on human studies. *Nat Rev Neurosci* 16:109–120.

9. Arendt T (2003) Synaptic plasticity and cell cycle activation in neurons are alternative effector pathways: The 'Dr. Jekyll and Mr. Hyde concept' of Alzheimer's disease or the yin and yang of neuroplasticity. *Prog Neurobiol* 71:83–248.
10. Arendt T, Stieler JT, Holzer M (2016) Tau and tauopathies. *Brain Res Bull* 126:238–292.
11. Freer R, et al. (2016) A protein homeostasis signature in healthy brains recapitulates tissue vulnerability to Alzheimer's disease. *Sci Adv* 2:e1600947.
12. Götz J, et al. (1995) Somatodendritic localization and hyperphosphorylation of tau protein in transgenic mice expressing the longest human brain tau isoform. *EMBO J* 14:1304–1313.
13. Goedert M, Jakes R, Crowther RA (1999) Effects of frontotemporal dementia FTDP-17 mutations on heparin-induced assembly of tau filaments. *FEBS Lett* 450:306–311.
14. Sperfeld AD, et al. (1999) FTDP-17: An early-onset phenotype with parkinsonism and epileptic seizures caused by a novel mutation. *Ann Neurol* 46:708–715.
15. Allen B, et al. (2002) Abundant tau filaments and nonapoptotic neurodegeneration in transgenic mice expressing human P301S tau protein. *J Neurosci* 22:9340–9351.
16. Hampton DW, et al. (2010) Cell-mediated neuroprotection in a mouse model of human tauopathy. *J Neurosci* 30:9973–9983.
17. Bellucci A, et al. (2004) Induction of inflammatory mediators and microglial activation in mice transgenic for mutant human P301S tau protein. *Am J Pathol* 165:1643–1652.
18. Woerman AL, et al. (2016) Tau prions from Alzheimer's disease and chronic traumatic encephalopathy patients propagate in cultured cells. *Proc Natl Acad Sci USA* 113:E8187–E8196.
19. Noble W, Hanger DP, Miller CCJ, Lovestone S (2013) The importance of tau phosphorylation for neurodegenerative diseases. *Front Neurol* 4:83.
20. Martin L, Latypova X, Terro F (2011) Post-translational modifications of tau protein: Implications for Alzheimer's disease. *Neurochem Int* 58:458–471.
21. Telling GC, et al. (1995) Prion propagation in mice expressing human and chimeric PrP transgenes implicates the interaction of cellular PrP with another protein. *Cell* 83:79–90.
22. Cabin DE, et al. (2005) Exacerbated synucleinopathy in mice expressing A53T SNCA on a Snca null background. *Neurobiol Aging* 26:25–35.
23. Dawson HN, et al. (2001) Inhibition of neuronal maturation in primary hippocampal neurons from tau deficient mice. *J Cell Sci* 114:1179–1187.
24. Lu PJ, Wulf G, Zhou XZ, Davies P, Lu KP (1999) The prolyl isomerase Pin1 restores the function of Alzheimer-associated phosphorylated tau protein. *Nature* 399:784–788.
25. Ando K, et al. (2013) Tau pathology modulates Pin1 post-translational modifications and may be relevant as biomarker. *Neurobiol Aging* 34:757–769.
26. Uchiyama K, et al. (2017) Prions amplify through degradation of the VPS10P sorting receptor sortilin. *PLoS Pathog* 13:e1006470.
27. Rogaeva E, et al. (2007) The neuronal sortilin-related receptor SORL1 is genetically associated with Alzheimer disease. *Nat Genet* 39:168–177.
28. Hu F, et al. (2010) Sortilin-mediated endocytosis determines levels of the frontotemporal dementia protein, progranulin. *Neuron* 68:654–667.
29. Kao AW, McKay A, Singh PP, Brunet A, Huang EJ (2017) Progranulin, lysosomal regulation and neurodegenerative disease. *Nat Rev Neurosci* 18:325–333.
30. Brady OA, Zheng Y, Murphy K, Huang M, Hu F (2013) The frontotemporal lobar degeneration risk factor, TMEM106B, regulates lysosomal morphology and function. *Hum Mol Genet* 22:685–695.
31. Campsall KD, Mazerolle CJ, De Repentingy Y, Kothary R, Wallace VA (2002) Characterization of transgene expression and Cre recombinase activity in a panel of Thy-1 promoter-Cre transgenic mice. *Dev Dyn* 224:135–143.
32. Braak H, Del Tredici K (2011) The pathological process underlying Alzheimer's disease in individuals under thirty. *Acta Neuropathol* 121:171–181.
33. Braak H, et al. (2003) Staging of brain pathology related to sporadic Parkinson's disease. *Neurobiol Aging* 24:197–211.
34. Mougenot A-L, et al. (2012) Prion-like acceleration of a synucleinopathy in a transgenic mouse model. *Neurobiol Aging* 33:2225–2228.
35. Luk KC, et al. (2012) Intracerebral inoculation of pathological α-synuclein initiates a rapidly progressive neurodegenerative α-synucleinopathy in mice. *J Exp Med* 209: 975–986.
36. Watts JC, et al. (2013) Transmission of multiple system atrophy prions to transgenic mice. *Proc Natl Acad Sci USA* 110:19555–19560.
37. Giasson BI, et al. (2002) Neuronal α-synucleinopathy with severe movement disorder in mice expressing A53T human α-synuclein. *Neuron* 34:521–533.
38. Andorfer C, et al. (2003) Hyperphosphorylation and aggregation of tau in mice expressing normal human tau isoforms. *J Neurochem* 86:582–590.
39. Ando K, et al. (2011) Accelerated human mutant tau aggregation by knocking out murine tau in a transgenic mouse model. *Am J Pathol* 178:803–816.
40. Wegmann S, et al. (2015) Removing endogenous tau does not prevent tau propagation yet reduces its neurotoxicity. *EMBO J* 34:3028–3041.
41. Nykjaer A, Willnow TE (2012) Sortilin: A receptor to regulate neuronal viability and function. *Trends Neurosci* 35:261–270.
42. Carlo A-S, et al. (2013) The pro-neurotrophin receptor sortilin is a major neuronal apolipoprotein E receptor for catabolism of amyloid-β peptide in the brain. *J Neurosci* 33:358–370.
43. Gustafsen C, et al. (2013) Sortilin and SorLA display distinct roles in processing and trafficking of amyloid precursor protein. *J Neurosci* 33:64–71.
44. Finan GM, Okada H, Kim T-W (2011) BACE1 retrograde trafficking is uniquely regulated by the cytoplasmic domain of sortilin. *J Biol Chem* 286:12602–12616.
45. Baker M, et al. (2006) Mutations in progranulin cause tau-negative frontotemporal dementia linked to chromosome 17. *Nature* 442:916–919.
46. Cruts M, et al. (2006) Null mutations in progranulin cause ubiquitin-positive frontotemporal dementia linked to chromosome 17q21. *Nature* 442:920–924.
47. Gass J, et al. (2006) Mutations in progranulin are a major cause of ubiquitin-positive frontotemporal lobar degeneration. *Hum Mol Genet* 15:2988–3001.
48. Fujimori F, Takahashi K, Uchida C, Uchida T (1999) Mice lacking Pin1 develop normally, but are defective in entering cell cycle from G(0) arrest. *Biochem Biophys Res Commun* 265:658–663.
49. National Research Council (2011) *Guide for the Care and Use of Laboratory Animals* (National Academies Press, Washington, DC), 8th Ed.
50. Chalkley RJ, Baker PR, Medzihradszky KF, Lynn AJ, Burlingame AL (2008) In-depth analysis of tandem mass spectrometry data from disparate instrument types. *Mol Cell Proteomics* 7:2386–2398.